First Flights of ER-2 X-band Radar - EXRAD

Gerald Heymsfield, Code 612, NASA/GSFC

The ER-2 X-band Doppler Radar (EXRAD) is a new radar that replaces the aging ER-2 Doppler Radar (EDOP) that has flown on the NASA ER-2 since 1992. EDOP has participated in numerous field campaigns for process studies and satellite validation and EXRAD will carry on some of this activity. EXRAD has all the capabilities of EDOP, except that it also has conical or cross-track scanning beam in addition to a nadir beam. The characteristics of EXRAD make it ideal for studying all types of precipitation systems.

Measurements:

- Radar reflectvity & Doppler velocity from nadir and scanning beams.
- 3D winds in precipitation regions.
- Ocean surface winds (scatterometry).

Instrument:

- Heritage: EDOP and CRS on the ER-2, originally designed for operation on Global Hawk.
- Single frequency X-band (9.6 GHz).
- Fixed nadir pointing beam and a cross track/conical scanning beam.
- Tube-based TWT transmitter.
- Funded for installation on ER-2 by NASA ESTO AITT, first test flights February 2013.

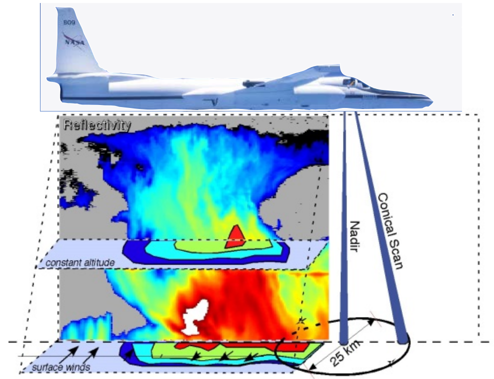

Figure 1. EXRAD measurement concept. Conical or cross-track scanning beam and nadir beam.

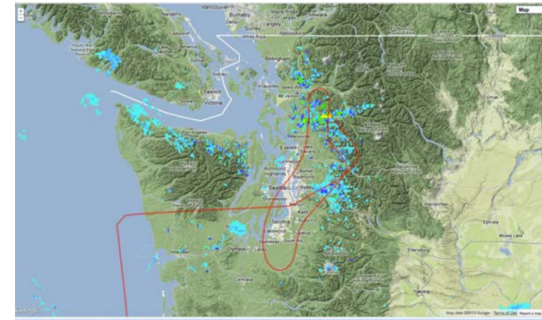

Figure 3. ER-2 flight track on 13 February 2013 over light precipitation and clouds near Seattle.

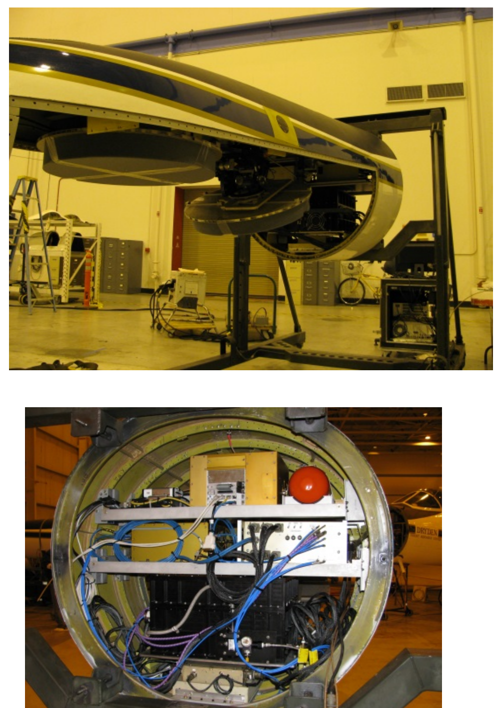

Figure 2: EXRAD installation in ER-2.

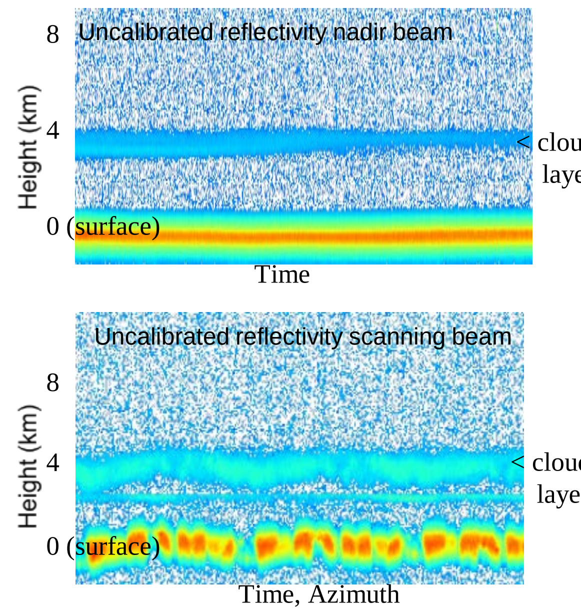

Figure 4. Cloud layer measured by EXRAD's nadir beam (top) and scanning beam (bottom). Red shades are high reflectivity surface, and lighter blue layer has radar reflectivity of about 20 dBZ.

Name: Gerald Heymsfield, NASA/GSFC, Code 612
E-mail: gerald.heymsfield@nasa.gov
Phone: 301-614-6369

Acknowledgement: We acknowledge Goddard IRAD support for EXRAD's early development. Support for installation of the instrument and test flights on the ER-2 were provided under ESTO-managed AITT 2010 program (L. Li, P.I., G. Heymsfield Co-P.I.).

Contributors: L. Li (GSFC), M. Mclinden (GSFC), J. Cervantes (SSAI), M. Perrine (GSFC), M. Coon (GSFC).

Technical Description of Figures:
The ER-2 X-band Radar (EXRAD) is a single-frequency radar that was originally developed for the Global Hawk prior to the High-altitude Imaging Wind and Rain Airborne Profiler (HIWRAP) instrument development. EXRAD was subsequently converted for use on the ER-2 aircraft since the ER-2 Doppler Radar (EDOP) was aging and becoming unreliable. EXRAD is a Doppler radar that measures radar backscatter at X-band (9.6 GHz). It is less affected in storms by attenuation that can be problematic in some regions for HIWRAP. EXRAD scanning antenna has capability for both azimuthal and elevation scan to provide both conical and cross-track scanning. The fixed nadir beam is similar to that on EDOP and it provides a direct measure of vertical hydrometeor motions from which vertical velocity can be derived. EXRAD recently competed test flights over very light rain in Washington state.

Figure 1: EXRAD measurement concept. The nadir-pointing beam provides high-resolution nadir "curtain" measurements below the plane from which reflectivity and vertical velocity can be derived in precipitation regions. After a wind retrieval, the scanning beam provides 3D structure of reflectivity and horizontal winds below the plane.
Figure 2: Pictures of the EXRAD antennas (top) and bulkhead section.
Figure 3: Flight path of the ER-2 during one of the test flights on February 14, 2013. The target was clouds and light precipitation near Seattle, WA.
Figure 4: Preliminary data from a cloud layer measured by EXRAD on February 14, 2013. The clouds and precipitation were very weak during this flight so there were only weak cloud layers in the data sets. The cloud layer in this figure is the thin blue feature at approximately 3.5 km altitude in both panels. The very thin layer below this cloud layer in the scanning beam (bottom panel) is an artifact resulting from leakage between the two beams.

Scientific significance: EXRAD provides a unique capability to study weather events such as deep convection and hurricanes, or other types of weather such as frontal systems. It has already been determined from previous HIWRAP measurements that attenuation and multiple scattering can be large in land-based severe storms with hail. EXRAD will be much less attenuated for these cases and can therefore provide less ambiguous information than the GPM frequencies for these extreme events. EXRAD flies in the ER-2 nose and can be part of a multi-sensor process oriented field campaign.

Relevance for future science and relationship to Decadal Survey: EXRAD will provide precipitation structure and winds that are important for process-oriented field campaigns, and for validation of satellite measurements. One example of the latter is the PACE decadal survey mission where the ER-2 along with EXRAD and a representative airborne radiometer can provide empirical relations between reflectivity or rain rate, with millimeter-wave radiometer brightness temperatures.

Particle shape matters for dust sedimentation and vertical structure

W. Yang, A. Marshak, T. Várnai, Code 613, NASA GSFC, A. Kostinski (Michigan Tech)

Dust aerosol has irregular shape, making its optical properties different from spherical aerosols. Does the particle shape also affect dust property variations along the altitude and their evolution during transport? Because particles of more irregular shape experience more air-resistance, their sedimentation may be slower, and so they may stay at higher altitudes for a longer time compared to spherical-like particles (Figure 1).

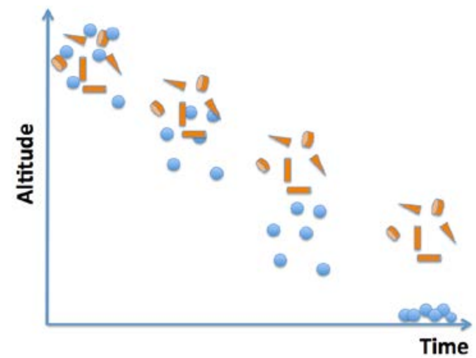

Figure 1. Schematic illustration of shape-dependent sedimentation. Spherical particles are blue while irregular shape (aspherical) particles are orange.

Recent CALIPSO observations on vertical distribution of Saharan dust particulate depolarization ratio (noted as δ hereafter) over 9 regions (Figure 2a) provide supportive evidence that dust shape does play an important role in sedimentation and consequently induces shape-dependent stratification during transport. δ is important as it can reveal particle irregularity. For example, while δ is close to zero for spherical particles, it is typically much larger for irregular dust particles.

The larger δ values at higher altitudes and higher δ lapse rate as dust leaves further away from its source (Figures 2b-2c) clearly indicate the progressive preponderance of aspherical particles at higher altitudes during westward transport (Figure 2d).

All these features can be captured qualitatively by a minimal model (two shapes only), suggesting that shape-dependent sedimentation and consequent stratification indeed contribute significantly to the observed temporal evolution and vertical stratification of dust properties. (We note that considering this stratification can help accurate estimations of dust radiative impacts.)

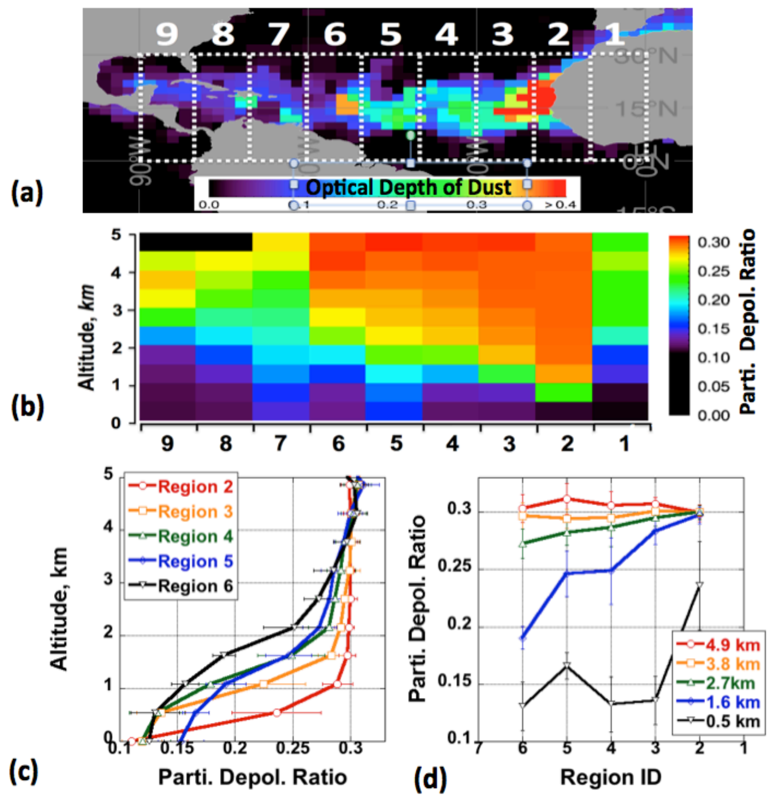

Figure 2. CALIPSO observation of Saharan dust along the westward transport path in summertime. (a) 9 consecutive regions studied. (b) vertical structure of particulate depolarization ratio, δ. (c) δ as a function of altitude. (d) δ as a function of longitude-regions.

Earth Sciences Division - Atmospheres

Name: Weidong Yang, NASA/GSFC Code 613
E-mail: Weidong.Yang@nasa.gov
Phone: 301-614-6226

References:

Yang, W., A. Marshak, T. Várnai, O. V. Kalashnikova, and A. B. Kostinski (2012), CALIPSO observations of transatlantic dust: vertical stratification and effect of clouds, Atmos. Chem. Phys., 12, 11339–11354

Yang, W., A. Marshak, A. B. Kostinsk, and T. Várnaii (2013), Shape-induced gravitational sorting of Saharan dust during transatlantic voyage: evidence from CALIOP lidar depolarization measurements., Geophysical Research Lett. (submitted March 2013).

Ginoux, P. (2003), Effects of nonsphericity on mineral dust modeling, J. Geophys. Res., 108(D2), 4052, doi:10.1029/2002JD002516,.

Data Sources: CALIPSO Level 2 aerosol and cloud products, June-August, 2007.

Technical Description of Figures:

Figure 1: Schematic illustration of shape-induced differential sedimentation: because of the higher settling speed of spherical particles, the initially localized group of spherical (blue) and aspherical (orange) particles (all at the same mass and volume), gradually separates, creating a stratified structure with the preponderance of aspherical particles at the top.

Figure 2: CALIPSO observation of Saharan dust along the path of westward transport in summertime. (a) Positioning of the 9 consecutive regions studied. Colors encode values of the median optical depth of dust layers at 2° by 2° horizontal resolution. (b) dust particle depolarization ratio, δ, as a function of altitude in the 9 regions. Colors represent the δ values. (c) dust δ as a function of altitude in Regions 2 to 6. (d) dust δ as a function of longitude-regions. The vertical resolution is 540 m. As the dust leaves the west coast of Africa (Region 2), the δ values at all altitudes above ~2 km are about the same but in the course of westward transport, the depolarization spreads out with higher ratios at higher altitudes. Furthermore, the depolarization ratio lapse rate increases westward. The altitude-independent δ in Region 2 indicates that particles of various shapes are randomly mixed throughout the atmospheric column. The progressive westward dispersion of δ suggests a separation of dust by shape-induced differential settling. The longer time causes wider vertical separation, and consequently, a higher lapse rate of the vertically increasing δ is observed with westward transport.

Scientific significance: By analyzing CALIPSO depolarization measurements, this study provides the first observational evidence that particle shape is a significant factor in the dust sedimentation process. Irregular dust particles settle slower than the more spherical-like ones, which leads to an inhomogeneous shape-dependent vertical structure with the preponderance of aspherical particles at higher altitudes. Since the light scattering properties of particles are strongly related to particle shape, our results imply that the dust optical properties are vertically inhomogeneous during transatlantic transport. Considering this stratification can help accurate estimations of dust radiative properties and radiative impacts.

Relevance for future science: Better understanding the inhomogeneity of dust properties and their distribution in space can help improve the accuracy of the retrievals of aerosol properties and therefore have implications on dust radiative forcing.

Attribution of sources of pollution to the Western Arctic during the NASA ARCTAS field campaign

Huisheng Bian, Code 614, NASA GSFC / UMBC JCET

Most of pollutants found in Arctic air have been transported from middle latitudes, and a large fraction is attributable to anthropogenic and biomass burning emissions. Local biomass burning is another important source of Arctic pollution. We use DC-8 airborne measurements of CO from ARCTAS-A and ARCTAS-B in combination with tagged CO tracers simulations in GEOS-5 to investigate potential pollutant sources and their transport to and within the Western Arctic.

Figure 1, a, b indicates that about 1/3 of the mean of the Western Arctic CO in both campaign periods came from background CO produced by CH_4 oxidation (i.e. the 'Other CO' in the figure). The remainder in April was mostly impacted by Asian Anthropogenic emissions, ASFF (accounting for more than 1/4 of the Arctic CO mean), and biomass burning (which contributed roughly 2/3 as much as ASFF). In July, both ASFF and Boreal Biomass Burning (BOBB) had comparable contributions to the mean CO. Biomass burning also made a large contribution to the variability of Arctic pollution in July. On the other hand, we found that European sources seldom made important contributions to the CO during the campaign domain and period.

Comparison of model results along flight tracks and over the whole Western Arctic region in Figure 1 c, d indicate that measurements during spring (ARCTAS A) are representative of the whole Western Arctic, but not during summer (ARCTAS B).

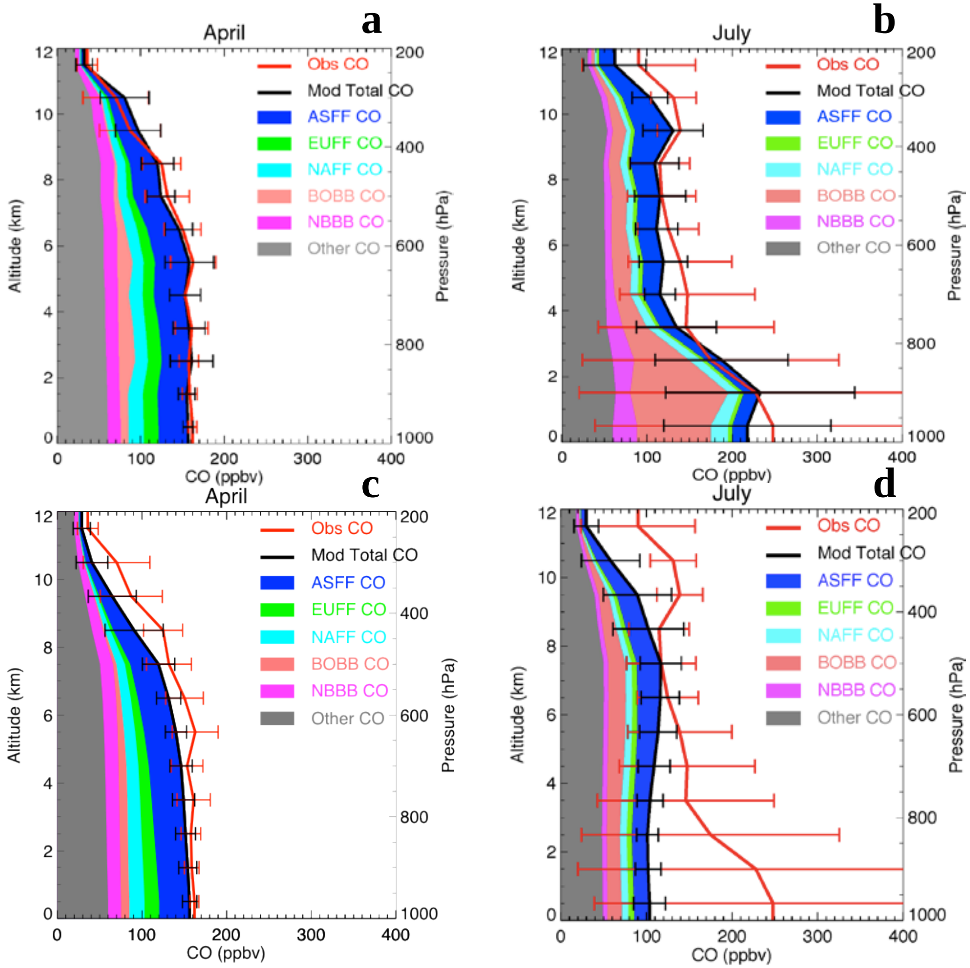

Figure 1: Vertical distribution of CO volume mixing ratio (ppbv) from DC-8 measurement and GEOS-5 simulation when the GEOS-5 model results are sampled by all flights for April (a) and July (b). The DC-8 CO along flight tracks is shown by the solid thick red line with standard deviation shown by horizontal bars. GEOS-5 CO is shown by the thick black line for total and by the color shaded areas for the five tag components (ASFF: Asian Anthropogenic, EUFF: European Anthropogenic, NAFF: North American Anthropogenic, BOBB: Boreal Biomass burning, NBBB: Non-boreal biomass, and 'Other CO': the global CO other than the five tagged COs. (c) and (d) Similar to (a) and (b) but the GEOS-5 model is the Arctic regional mean over 50N-90N and 190E-320E.

Name: Huisheng Bian
E-mail: Huisheng.Bian@nasa.gov
Phone: 301-614-5092

References:
H. Bian, P. Colarco, M. Chin, G. Chen, A.R. Douglass, J.M. Rodriguez, Q. Liang, et al.. Investigation of source attributions of pollution to the Western Arctic during the NASA ARCTAS field campaign. *Atmos. Chem. and Phys. Disc.*, 12, 8823-8855, 2012, (in review).

Data Sources: Aircraft measurements from NASA ARCTAS-A campaign (based on Fairbanks, Alaska during April, 2008) and ARCTAS-B campaign (based on Cold Lake, Canada during July, 2008); Model simulation results from NASA GEOS-5 tracer transport model running in $0.625^{\circ} \times 0.5^{\circ}$ resolution.

Technical Description of Figures:
Figure 1: Model results can be used in investigation of regional air pollution due to its spatial and temporal coverage and its capability in identifying pollution sources. To get confidence in this analysis, the model needs to be fully evaluated using in-situ measurements such as aircraft measurements. Figure 1a-b shows the evaluation of the NASA GEOS-5 model using NASA ARCTAS aircraft measurements by sampling the model results at the measurement time and location in the ARCTAS-A and B respectively. (Also shown in the paper the evaluation of the model capability in characterizing air mass origins by combining the model tagged CO tracers with the observed tracers CH_3CN (a biomass burning tracer) and CH_2Cl_2 (a fossil fuel tracer).) Figure 1c-d shows the application of the evaluated GEOS-5 model in investigating regional wide pollution in the Western Arctic in the ARCTAS-A and B respectively.

Scientific significance: The Arctic is a region particularly sensitive to climate change. There is an urgent need to better understand changes in Arctic atmospheric composition and its feedback on climate: Potential warming of the Arctic could reduce ice cover and release methane from permafrost, both of which would accelerate global warming. Meanwhile, studying pollution over the Arctic has implications for regulation purpose since the Arctic serves as an important indicator of remote environmental changes because the effects of pollution from distant sources are clearly discernible. This study combines the advantages of the NASA GEOS-5 model simulation and the NASA ARCTAS campaign measurements to investigate the source attribution of pollution to the Western Arctic during the NASA ARCTAS field campaign, which constitutes a piece of an international effort of studying Arctic pollution during the International Polar Year in 2007-2008. Our study indicates that Asian anthropogenic pollution has become a dominate foreign source transported to the Western Arctic.

Relevance for future science and relationship to Decadal Survey: Studying the Arctic is challenging partially due to lack of measurements there from traditional passive instruments such as MODIS and MISR onboard NASA satellites. Lidar technology used in current satellite CALIPSO and future satellite ACE will fill this gap but the potential contamination due to the Arctic complex surface conditions needs to be addressed. A carefully evaluated model (e.g. GEOS-5) by in-situ ground and aircraft measurements is useful to properly interpret the satellite measurements over the Arctic .